

***L*-edge resonant magneto-optical Kerr effect of a buried Fe nanofilm**Y. Kubota,¹ M. Taguchi,² H. Akai,¹ Sh. Yamamoto,¹ T. Someya,¹ Y. Hirata,¹ K. Takubo,¹ M. Araki,¹ M. Fujisawa,¹ K. Yamamoto,¹ Y. Yokoyama,¹ S. Yamamoto,¹ M. Tsunoda,³ H. Wadati,¹ S. Shin,¹ and I. Matsuda^{1,*}¹*Institute for Solid State Physics, The University of Tokyo, Kashiwa-no-ha, Kashiwa, Chiba 277-8581, Japan*²*Nara Institute of Science and Technology (NAIST), Ikoma, Nara 630-0192, Japan*³*Department of Electronic Engineering, Tohoku University, Sendai 980-8579, Japan*

(Received 30 June 2016; revised manuscript received 15 July 2017; published 30 October 2017)

The Fe *L*-edge resonant magneto-optical Kerr effect of a buried Fe nanofilm was investigated by rotating-analyzer ellipsometry and the results were compared with those from three theoretical simulations. The reversal of the Kerr rotation angle θ_K between the L_3 and L_2 edges, observed in the experiment, was consistent with classical electromagnetic simulation using empirical optical constants. The spectral θ_K feature was reproduced by the first-principles calculation of the KKR-Green's function method on the itinerant electronic system. The demonstration indicates that spectra of the *L*-edge resonant MOKE can be understood in terms of both the macroscopic and microscopic pictures.

DOI: [10.1103/PhysRevB.96.134432](https://doi.org/10.1103/PhysRevB.96.134432)**I. INTRODUCTION**

Magnetism is a central subject in condensed matter physics with many magnetic properties of materials being measured experimentally using magneto-optical effects, such as the Faraday effect [1,2] and the magneto-optical Kerr effect (MOKE) [3,4]. In MOKE measurements, the rotation of the light polarization plane is measured before and after reflection at a sample surface. The change of the polarization angle is defined as the Kerr rotation angle θ_K , which depends on the magnetization of the sample. When measured with visible light, the value of θ_K typically is < 1 degree for the bulk crystals of magnetic transition metals, such as Fe, Co, and Ni [5]. On the other hand, recent reports indicated that the θ_K values become significantly large in the ultraviolet to x-ray region when a probing photon energy is tuned at the absorption edge of a magnetic element in the sample [6–13]. The phenomenon, referred to as resonant MOKE (RMOKE), has enabled the magnetic properties of a material to be evaluated with element-selectivity. This effect looks promising as a probe to study magnetism and spin dynamics using synchrotron radiation, x-ray free electron laser, and high-harmonic generation laser.

For RMOKE of an Fe film, the experimental θ_K value is 10° at the L_3 and L_2 photon energy regions [8,9]. From theory, analysis from the first-principles calculation indicates that θ_K is $\sim 50^\circ$ when the photon energy is at the Fe L_2 edge for the Fe-metal bulk crystal [14]. This theoretical θ_K value exceeds the light phase shift of $\pi/4$ that corresponds to the variation of light polarization from linear to circular. RMOKE has the potential to be applied in the field of optical manipulation. Such light control using the magneto-optical effect in the soft x-ray region has already been proposed [15–17]. However, there still remains a discrepancy in the θ_K values between experiment and theory that requires a systematic comparison of RMOKE spectra for a proper understanding of the magneto-optical phenomena.

In the present study, we examine the *L*-edge RMOKE for a buried Fe nanofilm by comparing θ_K spectra obtained

by measurement and by calculations using three theoretical models, one from classical electromagnetics and the other two from quantum mechanics. In the measured RMOKE spectra, negative and positive θ_K peaks were observed at L_3 and L_2 edges, respectively. The θ_K values and the change of sign at the $L_{2,3}$ edges were reproduced fairly well in the classic electromagnetic simulation with empirical optical constants obtained from a previous diffraction experiment [18].

One of the quantum mechanics calculations treated the resonant scattering with the itinerant Fe electronic bands that were derived by the density functional theory. With the KKR-Green's function method, the simulated spectra reproduce the experimental result, including the θ_K reversal. On the other hand, the other quantum mechanics calculation was based on resonant scattering theory with the localized electrons in the configuration interaction (CI) model that has been adopted conventionally in analyzing soft x-ray spectra. The calculated θ_K value at the L_2 edge reached 48° , which reproduced the previous theoretical result [14]. However, it was much larger than the experimental θ_K and the simulated spectrum showed the nonreversal feature, which was also distinct from the measured one. The consistency and discrepancy between experiment and theories settles the conventional arguments on interpretations of the *L*-edge resonant scattering of transition metals. Moreover, the research provides the appropriate theoretical model to make the microscopic interpretation in an *L*-edge RMOKE spectrum.

II. EXPERIMENT

Figure 1(a) shows a schematic drawing of the heterostructure of the Ta/Cu/Fe/MgO sample. A 30-nm-thick Fe film was epitaxially grown on the MgO(001) substrate by magnetron sputtering. It was then capped with Ta (2-nm-thick) and Cu (2-nm-thick) layers to prevent the Fe layer from oxidization. The buried Fe nanofilm has an in-plane easy direction of magnetization. RMOKE measurements were made at the SPring-8 BL07LSU beamline [19] with the geometric setup for longitudinal MOKE (L-MOKE), as shown in Fig. 1(b). Photon energies at the Fe L_3 and L_2 edges were determined from x-ray absorption spectroscopy (XAS) of the same sample.

*imatsuda@issp.u-tokyo.ac.jp

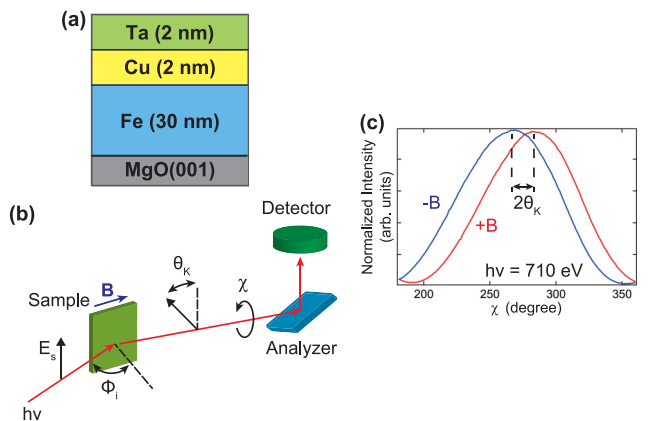


FIG. 1. (a) Schematic of the 30-nm-thick Fe film on the MgO(001) substrate. Ta (2 nm) and Cu (2 nm) are capping layers. (b) Setup of the L-MOKE measurement with RAE. RAE comprises by a multimirror and a MCP. (c) Typical results of the intensity variation with rotation angle, χ , taken at $h\nu = 710$ eV. The red and blue solid lines represent the spectra obtained when the magnetic fields were $+0.3$ T ($+B$) and -0.3 T ($-B$), respectively. The Kerr rotation angle can be determined from $2\theta_K = \theta(-B) - \theta(+B)$.

The s -polarized light illuminated the sample at an incident angle (ϕ_i) of about 80° with respect to the surface normal. A magnetic field (B) of ± 0.3 T was applied along the in-plane direction of the sample surface. The strength of the field is large enough to saturate the Fe magnetization.

The θ_K values were obtained by the rotating-analyzer ellipsometry (RAE). The RAE unit was composed of a multimirror and a microchannel plate (MCP), as shown in Fig. 1(b). In brief, θ_K can be determined from the difference in the ellipsometry curves taken under opposite magnetic fields: $2\theta_K = \theta(-B) - \theta(+B)$, as shown in Fig. 1(c). Details of the measurement technique can be found elsewhere [12].

III. RESULT AND DISCUSSION

The θ_K spectrum for a buried Fe nanofilm taken at the Fe $L_{2,3}$ edges shows negative (about -18°) and positive (about 7°) values at the L_3 and L_2 absorption edges, respectively, as shown in Fig. 2(a).

A. Simulation based on classical electromagnetic calculation with empirical parameters

Based on classical electromagnetic theory, θ_K and the ellipticity (ε_K) for the s -polarized mode are expressed by the complex Fresnel coefficients r_{ss} and r_{ps} [3,8,9]:

$$\theta_K + i\varepsilon_K = -r_{ps}/r_{ss} \approx \frac{-in_0Q}{(n^2 - n_0^2)} \left(\frac{\cos \phi_i \tan \phi_t}{\cos(\phi_i - \phi_t)} \right), \quad (1)$$

where n and n_0 represent the complex refraction constants of the Fe film and the capping layer, respectively, which individually are given as $n = 1 - \delta_1 + i\beta_1$ and $n_0 = 1 - \delta_0 + i\beta_0$. Therefore, in applying the model for a buried Fe film, the optical properties of both the film and the overlayer need to be considered. The constant, $n(n_0)$, is composed of a real part $1 - \delta_{1(0)}$ and an imaginary part $\beta_{1(0)}$ that represent nonmagnetic dispersion and absorption, respectively. The

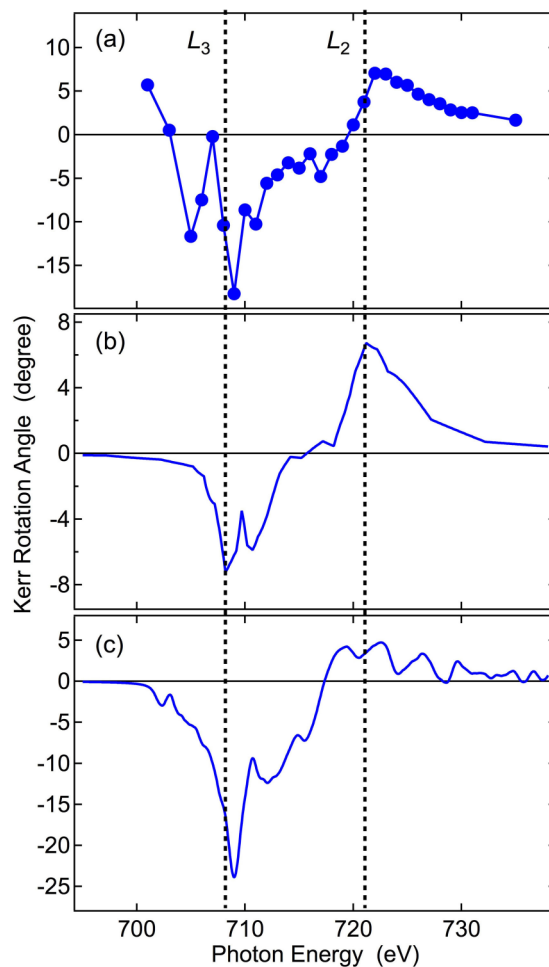


FIG. 2. Spectra of the magneto-optical Kerr rotation angle θ_K of the buried Fe nanofilm at Fe $L_{2,3}$ edges obtained by (a) measurement and (b) classical electromagnetic calculation with empirical optical constants. (c) A simulated spectrum of the quantum-mechanical calculation on Fe metal with the KKR-Green's function method. Two dashed lines correspond to the L_2 and L_3 absorption edges. Experimental errors are smaller than a size of the data points, represented as solid circles.

Voigt parameter Q for the L-MOKE geometry is given by $Q = (n_+ - n_-)/(n \sin \phi_t)$ where ϕ_t is the angle of refraction and n_{\pm} are the magneto-optical constants with $n = 1/2(n_+ + n_-)$. The latter are written $n_{\pm} = 1 - (\delta_1 \pm \Delta\delta) + i(\beta_1 \pm \Delta\beta)$, where the subscripted sign \pm indicates that the directions of the photon helicity and magnetization are parallel/antiparallel in the sample. Here, $\Delta\delta$ and $\Delta\beta$ denote the magnetic contributions of δ_1 and β_1 , respectively. When ϕ_i is large ($70^\circ \leq \phi_i \leq 90^\circ$) and $\phi_i \approx \phi_t$, Eq. (1) can be rewritten as

$$\theta_K + i\varepsilon_K \approx \frac{-in_0(n_+ - n_-)}{(n^2 - n_0^2)}. \quad (2)$$

The average index $\delta_{\text{Ta/Cu}}$ ($\beta_{\text{Ta/Cu}}$) of the Ta/Cu capping layer can be obtained from the δ_{Ta} (β_{Ta}) and δ_{Cu} (β_{Cu}) of the individual layers Ta and Cu with relative Ta amount,

$$\gamma = d_{\text{Ta}}/(d_{\text{Ta}} + d_{\text{Cu}}),$$

$$\delta_{\text{Ta/Cu}} = \gamma\delta_{\text{Ta}} + (1 - \gamma)\delta_{\text{Cu}}, \quad (3)$$

$$\beta_{\text{Ta/Cu}} = \gamma\beta_{\text{Ta}} + (1 - \gamma)\beta_{\text{Cu}}, \quad (4)$$

where d_{Ta} (d_{Cu}) represents the thickness of the Ta (Cu) capping layer [18]. The indices δ and β of Fe were taken from a result obtained from a resonant magnetic Bragg scattering experiment on a Fe/C multilayer [18], while those of other materials were taken from tabulated values given in the reference [20]. Interpolations of the data points were done to improve the quantitative comparison with the experimental data. Note that a θ_K value determined by a previous L-MOKE measurement [8,9] on the Al-capped Fe film was likely to have been considerably affected by a large diverging value for factor $1/(n^2 - n_{\text{Al}}^2)$ in Eqs. (1) and (2) because the square of the refraction constants, n^2 and n_{Al}^2 , are almost identical at photon energies around the L_2 and L_3 absorption edges [8,9]. As $n_{\text{Ta/Cu}}^2$ is much away from n^2 of Fe in any photon energy range, θ_K determined with the Ta/Cu-capped Fe film in this study should succeed in removing the effect of the capping layers and be closer to the inherent value of Fe than one with a Al/Fe sample [8,9], resulting in the first observation of the sign change.

In Fig. 2(b), a curve of the θ_K spectral simulation, based on the experimental optical constants [18,20] and Eq. (2), is shown. Compared with the measured value in Fig. 2(a), one finds that the two results of the experiment and the calculation match

well overall, reproducing the sign inversion of θ_K between the L_2 and L_3 absorption edges. On the other hand, a dip structure can be found at the L_3 edge in the experimental spectrum in Fig. 2(a). The spectral dip has also been reported in the previous RMOKE experiment [8,9] on the magnetic nanofilms and it has been discussed to be the result of optical interference by the interfaces of the film. It is inferred that the dip structure may depend on the film structure of a sample and the reference parameter, obtained from different samples and different instruments with different energy resolution, may not be sufficient to reproduce the detailed features by the current simulation.

B. The first-principles calculation based on quantum resonant scattering theory on the itinerant electronic system

The θ_K spectra for the *bcc* bulk Fe crystal were calculated by the KKR-Green's function method using Machikaneyama (AkaiKKR), a KKR-CPA-LDA package [21]. In the present first-principles calculation, the itinerant Fe band structure was obtained within the framework of local-density-approximation (LDA) of the density functional theory. The cores and valence states were calculated including the relativistic effects. Details of the calculation method can be found elsewhere [22]. As shown in Fig. 2(c), the calculated θ_K spectrum shows the sign reversal and, moreover, it is quantitatively consistent with the experimental one in Fig. 2(a). Figure 3 summarizes spectra of θ_K and ε_K of the *bcc* bulk Fe crystal at the Fe $L_{2,3}$ edges. Spectra of θ_K and ε_K are related to each

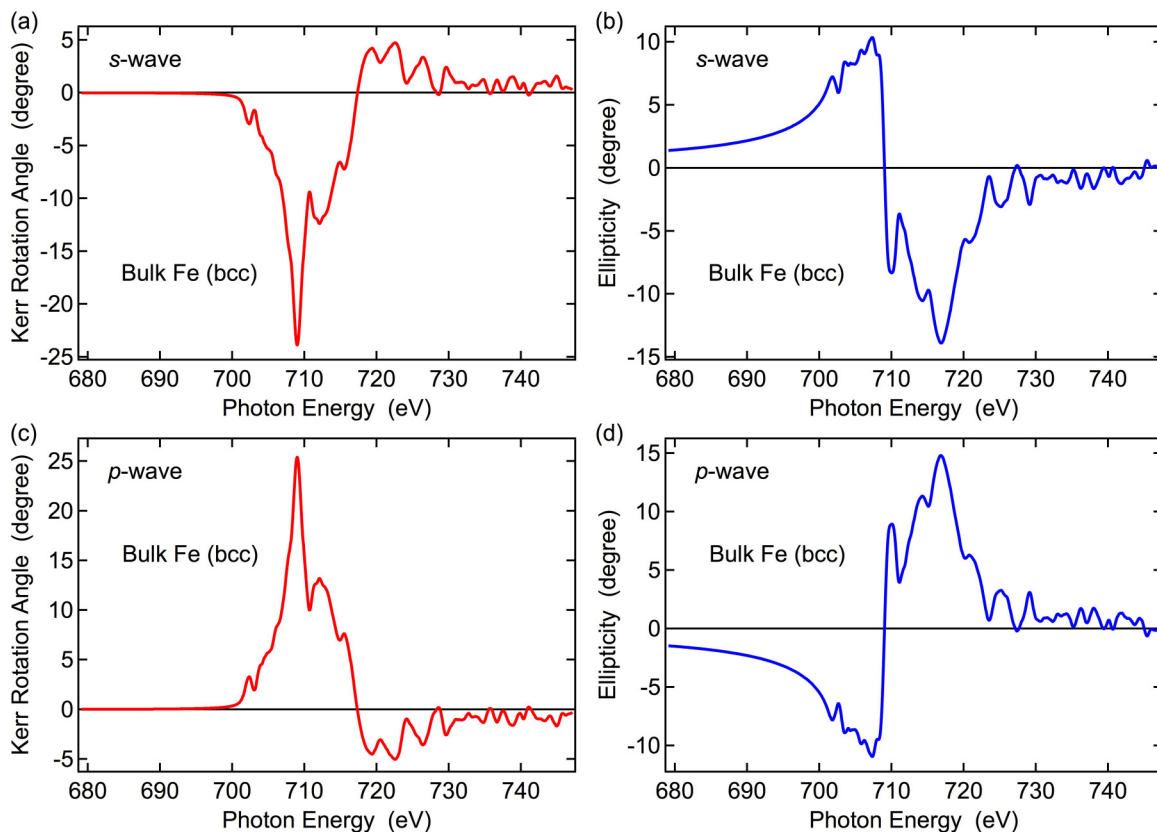


FIG. 3. Spectra of θ_K and ε_K of the Fe metal at the Fe $L_{2,3}$ edges obtained by the quantum-mechanical calculation with the KKR-Green's function method at [(a) and (b)] the *s*-wave and [(c) and (d)] the *p*-wave configurations.

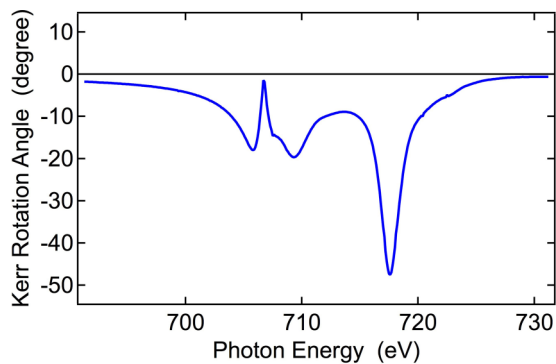


FIG. 4. Spectra of θ_K of the Fe metal at the Fe $L_{2,3}$ edges obtained by the quantum-mechanical calculation with the CI model.

other through the Kramers-Kronig relations. The signs of the spectra invert when the measurement configuration changes between the s wave [Figs. 3(a) and 3(b)] and the p wave [Figs. 3(c) and 3(d)] due to the definition reason. These spectral features self-consistently indicate the appropriateness of the calculation. Concerning the detailed spectral features, such as a dip at the L_3 edge, one finds there are discrepancies between the experiment and the calculation. This is actually consistent with the previous assignment [8,9] that the fine

structures originate from the macroscopic picture, such as the optical interference by interfaces of the film, which were not included in the calculation of the ideal bulk Fe metal. Consequently, the present first-principles calculation indicates it is the microscopic picture that reproduces the spectral sign reversal in the θ_K spectra.

C. Simulation based on quantum resonant scattering theory on the localized electronic system

In the present research, we examine the other quantum theoretical calculation with a CI model based on a localized Anderson impurity approach, where both the many-body charge transfer effect and intra-atomic multiplet interactions are taken into account. This quantum-mechanical spectral calculation has been typically made for simulating soft XAS and resonant scattering data. In the following, we briefly describe the model adopted for L edge in this study. Further details can be found in the previous papers [12,23–25].

In the calculation, we select a central Fe atom with appropriate linear combinations of $3d$ orbitals on neighboring sites to serve as a reservoir of holes, here denoted by \underline{L} . The Hamiltonian contains two terms $H_0 + T$. The H_0 describes the localized Anderson impurity model including intra-atomic multiplet interaction and interatomic hybridization V . The electric-dipole transition operator T leads to $2p \rightarrow 3d$ XAS.

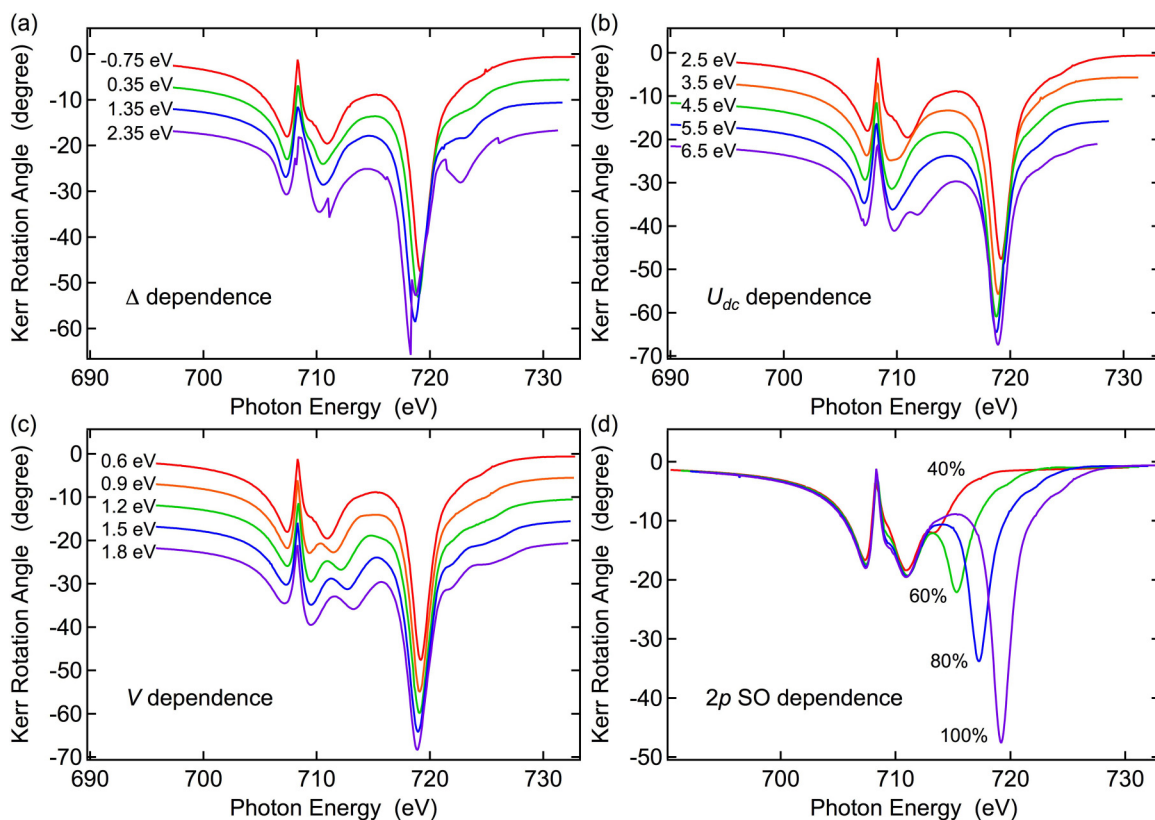


FIG. 5. (a) Δ dependence of θ_K spectra obtained by the CI model calculation. The red, green, blue, and purple lines represent $\Delta = -0.75, 0.35, 1.35,$ and 2.35 eV, respectively. (b) U_{dc} dependence of θ_K spectra. The red, orange, green, blue, and purple lines represent $U_{dc} = 2.5, 3.5, 4.5, 5.5,$ and 6.5 eV, respectively. (c) V dependence of θ_K spectra. The red, orange, green, blue, and purple lines represent $V = 0.6, 0.9, 1.2, 1.5,$ and 1.8 eV, respectively. These spectra are vertically shifted for clarification by 5° . (d) θ_K spectra obtained by the CI model calculation depending on the SO strength of the $2p$ electron. The red, green, blue, and purple lines represent 40, 60, 80, and 100% of the $2p$ SO value for an isolated Fe atom, respectively.

We describe the ground state of these systems by a linear combination of three configurations, $3d^n$, $3d^{n+1}\underline{L}$, and $3d^{n+2}\underline{L}^2$. The intermediate states are thus described by linear combinations of $2p^53d^{n+1}$, $2p^53d^{n+2}\underline{L}$, and $2p^53d^{n+3}\underline{L}^2$. The final state contains $3d^n$, $3d^{n+1}\underline{L}$, and $3d^{n+2}\underline{L}^2$. For the ground state, we used the following parameters: charge transfer energy (Δ) = -0.75 eV, on-site Coulomb interaction between $3d$ states (U_{dd}) = 1.5 eV, core-hole potential (U_{dc}) = 2.5 eV, and hybridization energy (V) = 1.6 eV. The spin-orbit (SO) strength of the $2p$ and $3d$ electrons in the Fe nanofilm are set as the isolated Fe atom (SO_{atom}), if not specified. The Slater integrals (Racah parameter) required to evaluate the parameters are calculated using the Hartree-Fock method and rescaled by 85% [26,27]. The θ_K spectrum is calculated using the Kramers-Heisenberg formula [12,23–25].

Figure 4 shows the result of the quantum-mechanical spectral calculation with the CI model. The spectrum has a large θ_K peak of $\sim 48^\circ$ between the L_3 and L_2 edges (Fig. 4) and it does not show a sign inversion between the Fe L edges. Though this feature does not match with the experimental spectrum [Fig. 2(a)], the large θ_K peak reproduces a result of the previous quantum mechanical calculation ($\sim 50^\circ$) [14]. This result indicates that the conventional theoretical approach of the CI model is not appropriate to simulate the whole the L -edge spectra of the Fe metal. In order to understand the origin of these spectral features, Figs. 5(a)–5(c) show a collection of the θ_K spectra with various values of Δ , U_{dc} , and V . Besides the faint features in the spectra that depend on these parameters, one can find that the large peak are found under all the conditions. Thus, the main feature does not reflect the electronic states of a material. It is inferred that the spectral structure is resulted from the complex (quantum) superposition of wave functions of the (Fe $2p$ -Fe $3d$) resonant elastic scattering in the Kramers-Heisenberg formula. Recent research of the resonant x-ray emission spectroscopy (RXES) also pointed out necessity to consider such a quantum effect in a process of the resonant inelastic scattering to make a proper interpretation for the magnetic circular dichroisms in the RXES spectra [28]. Making the investigations further, we virtually change the SO strength of the $2p$ electrons in the Fe nanofilm, as shown in Fig. 5(d). Reducing the SO strength from SO_{atom} (100%), one can find a drastic variation of the large θ_K peak. This indicates a close relation between the spectral peak and the atomic orbital. It is of note that the variation on the SO strength of the $3d$ electrons does not show any apparent change in spectra. Taking also into account that the large peak was absent in the calculated results of the itinerant electronic

system (Fig. 3), it seems it is the localized electron model that leads to large discrepancy between the experiment and the calculation.

IV. SUMMARY

In the present research, we comprehensively studied the Fe L -edge resonant MOKE spectrum of the Fe film by experiment and by simulations of the three theoretical models. The θ_K spectrum that shows the sign inversion between the L_3 and L_2 edges is reproduced by the classical electromagnetism simulation with the empirical optical constants. The spectrum also matched with the results of the first-principles calculation of the KKR-Green's function method on the Fe itinerant $3d$ electronic system. On the other hand, the conventional theoretical calculation of the CI model shows a different MOKE spectrum with a peak of the large θ_K value that seems to originate from the calculation with the atomic Fe $3d$ orbitals. A series of the data in the present research reveals the necessity to consider the delocalized $3d$ states in the transition metal and demonstrates the validity of the KKR-Green's function approach to simulate the magneto-optical effect at the absorption edges. A combination of this first-principles calculation and the resonant MOKE experiment provides an accurate microscopic picture of the element-specific magnetic moments and the itinerant electronic states in magnetic phenomena.

ACKNOWLEDGMENTS

This work was partially supported by the Ministry of Education, Culture, Sports, Science, and Technology of Japan (X-ray Free Electron Laser Priority Strategy Program and Photon and Quantum Basic Research Coordinated Development Program), the Japan Society for the Promotion of Science grant-in-aid for Scientific Research (C) (Grant No. 26400328), and the Asahi Glass Foundation. The experiment was performed using facilities of the Synchrotron Radiation Research Organization, The University of Tokyo (Proposal Nos. 2014A7401, 2014B7401, 2014B7473, 2015A7401). We thank M. Kotsugi for valuable discussion and H. Narita for building the experimental equipment. V. Lollobrigida is acknowledged for his support during the experiment. M.T. acknowledges H. Daimon for supporting his research by valuable discussion. Y.K. acknowledges support from the ALPS programs of the University of Tokyo.

-
- [1] H.-C. Mertins, F. Schäfers, X. Le Cann, A. Gaupp, and W. Gudat, *Phys. Rev. B* **61**, R874 (2000).
 - [2] J. Kunes, P. M. Oppeneer, H.-C. Mertins, F. Schäfers, A. Gaupp, W. Gudat, and P. Novák, *Phys. Rev. B* **64**, 174417 (2001).
 - [3] P. M. Oppeneer, in *Handbook of Magnetic Materials*, edited by K. H. J. Buschow (Elsevier, Amsterdam, 2001), Vol. 13.
 - [4] Z. Q. Qiu and S. D. Bader, *Rev. Sci. Instrum.* **71**, 1243 (2000).
 - [5] H. Burkhard and J. Jaumann, *Z. Phys.* **235**, 1 (1970).
 - [6] J. B. Kortright, D. D. Awschalom, J. Stöhr, S. D. Bader, Y. U. Idzerda, S. S. P. Parkin, I. K. Schuller, and H.-C. Siegmann, *J. Magn. Magn. Mater.* **207**, 7 (1999).
 - [7] K.-S. Lee, S.-K. Kim, and J. B. Kortright, *Appl. Phys. Lett.* **83**, 3764 (2003).
 - [8] H.-C. Mertins, S. Valencia, D. Abramsohn, A. Gaupp, W. Gudat, and P. M. Oppeneer, *Phys. Rev. B* **69**, 064407 (2004).
 - [9] S. Valencia, H.-C. Mertins, D. Abramsohn, A. Gaupp, W. Gudat, and P. M. Oppeneer, *Phys. B Condens. Matter* **345**, 189 (2004).
 - [10] S.-K. Kim, K.-S. Lee, J. B. Kortright, and S.-C. Shin, *Appl. Phys. Lett.* **86**, 102502 (2005).
 - [11] M. F. Tesch, M. C. Gilbert, H.-C. Mertins, D. E. Bürgler, U. Berges, and C. M. Schneider, *Appl. Opt.* **52**, 4294 (2013).

- [12] Sh. Yamamoto, M. Taguchi, M. Fujisawa, R. Hobara, S. Yamamoto, K. Yaji, T. Nakamura, K. Fujikawa, R. Yukawa, T. Togashi, M. Yabashi, M. Tsunoda, S. Shin, and I. Matsuda, *Phys. Rev. B* **89**, 064423 (2014).
- [13] Sh. Yamamoto, M. Taguchi, T. Someya, Y. Kubota, S. Ito, H. Wadati, M. Fujisawa, F. Capotondi, E. Pedersoli, M. Manfreda, L. Raimondi, M. Kiskinova, J. Fujii, P. Moras, T. Tsuyama, T. Nakamura, T. Kato, T. Higashide, S. Iwata, S. Yamamoto, S. Shin, and I. Matsuda, *Rev. Sci. Instrum.* **86**, 083901 (2015).
- [14] H. J. Gotsis and P. Strange, *J. Magn. Magn. Mater.* **140-144**, 2171 (1995).
- [15] D.-E. Jeong, K.-S. Lee, and S.-K. Kim, *Appl. Phys. Lett.* **88**, 181109 (2006).
- [16] D.-E. Jeong and S.-K. Kim, *Phys. Rev. B* **78**, 012412 (2008).
- [17] D.-E. Jeong and S.-K. Kim, *J. Appl. Phys.* **105**, 07E709 (2009).
- [18] H.-C. Mertins, O. Zaharko, A. Gaupp, F. Schäfers, D. Abramsohn, and H. Grimmer, *J. Magn. Magn. Mater.* **240**, 451 (2002).
- [19] S. Yamamoto, Y. Senba, T. Tanaka, H. Ohashi, T. Hirono, H. Kimura, M. Fujisawa, J. Miyawaki, A. Harasawa, T. Seike, S. Takahashi, N. Nariyama, T. Matsushita, M. Takeuchi, T. Ohata, Y. Furukawa, K. Takeshita, S. Goto, Y. Harada, S. Shin, H. Kitamura, A. Kakizaki, M. Oshima, and I. Matsuda, *J. Synchrotron Radiat.* **21**, 352 (2014).
- [20] L. Henke, E. Gullikson, and J. C. Davis, http://www-cxro.lbl.gov/optical_constants/asf.html.
- [21] H. Akai, <http://kkr.issp.u-tokyo.ac.jp>.
- [22] H. Akai, *J. Phys.: Condens. Matter* **1**, 8045 (1989).
- [23] M. Taguchi, L. Braicovich, F. Borgatti, G. Ghiringhelli, A. Tagliaferri, N. B. Brookes, T. Uozumi, and A. Kotani, *Phys. Rev. B* **63**, 245114 (2001).
- [24] M. Taguchi, J. C. Parlebas, T. Uozumi, A. Kotani, and C.-C. Kao, *Phys. Rev. B* **61**, 2553 (2000).
- [25] M. Taguchi and G. van der Laan, *Phys. Rev. B* **66**, 140401 (2002).
- [26] R. Cowan, *Theory of Atomic Structure and Spectra* (University of California Press, Berkeley, 1981).
- [27] F. M. F. de Groot, *J. Electron Spectrosc. Relat. Phenom.* **67**, 529 (1994).
- [28] K. Fukui, H. Ogasawara, A. Kotani, T. Iwazumi, H. Shoji, and T. Nakamura, *J. Phys. Soc. Jpn.* **70**, 3457 (2001).